Scattering Tomography by Monte Carlo Voting

Yasunori Ishii†, Toshiya Arai†, Yasuhiro Mukaigawa‡,
Jun'ichi Tagawa†, Yasushi Yagi‡

† Panasonic Corporation, Japan, ‡ ISIR, Osaka University, Japan
†{*ishii.yasunori,arai.toshiya,tagawa.junichi*}*@jp.panasonic.com*,
‡ {*mukaigaw,yagi*}*@am.sanken.osaka-u.ac.jp*

Abstract

In this paper, we propose a new tomography method called Monte Carlo Voting to visualize the cross-sectional surfaces of scattering media. Since the incident light repeats a collision with small particles in scattering media, there are many light paths. To trace them, we use the Monte Carlo ray tracing algorithm and compute the attenuation ratio that represents the likelihood of hidden objects for each light path. The distribution of hidden objects is estimated by voting the attenuation ratio along the light path. Monte Carlo Voting statistically solves the tomography problem by combining Monte Carlo ray tracing and the voting process. Experiments using simulated and real images show that the distribution of hidden objects can be roughly estimated even when strong scatterings are observed.

1. Introduction

Technologies that visualize the inside of physical bodies are crucial in product inspections and medical diagnosis and are needed to detect foreign substances in food and needles in bodies, etc. Computed tomography is a widely used method to visualize the cross-sectional surfaces. X-ray CT yields clean images, but humans may be exposed to X-rays. Diffuse optical tomography (DOT) [1] using near-infrared light is safe but the images get blurred easily due to light scattering. Since it is very difficult to accurately model the light transport, approximate models are often used, based on the assumption of isotropic distribution.

On the other hand, when the optical density of a scattering media is low, some methods have been proposed to sharpen images by removing the scattering light, including a method to reduce scattering light using polarizer [6], a method of projecting high-frequency patterns [5], and a method to apply a single scattering model [4]. The angular filtering [2] successfully restored an internal three-dimensional structure by descattering using a pinhole array and by combining the visual hull algorithms. However, the above methods are only applied in situation that scattering light is small.

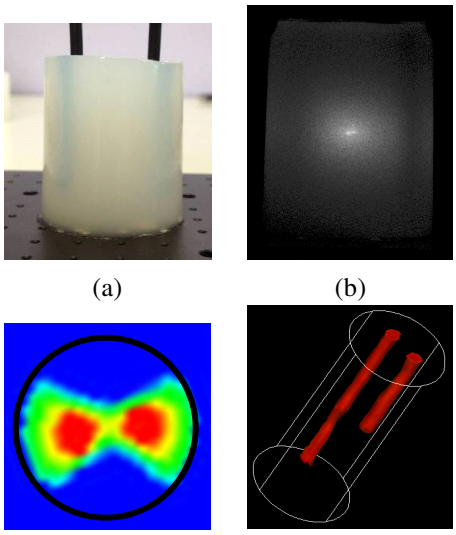

Figure 1: Tomography of two hidden objects in scattering media: (a) scattering media with hidden objects; (b) captured image of (a) illuminated by laser in darkroom; (c) estimated result by Monte Carlo Voting; (d) 3-D reconstruction result.

In this paper, we propose a new scattering tomography technology called the Monte Carlo Voting method that can be applied where light scatters at a high intensity. This method can estimate the distribution of hidden objects in scattering media because the light transport changes depending on their existence. The light transport within a scattering media is accurately simulated by Monte Carlo ray tracing. The distribution of the hidden objects is statistically estimated by voting.

The following are the contributions of our proposed method: (1) We formulated the inverse problem of a scattering by Monte Carlo ray tracing, which is faithful to a physical phenomenon without using approximate models. (2) With the voting process, we clarified that the distribution of hidden objects can be stably estimated, while it tends to be ill-posed.

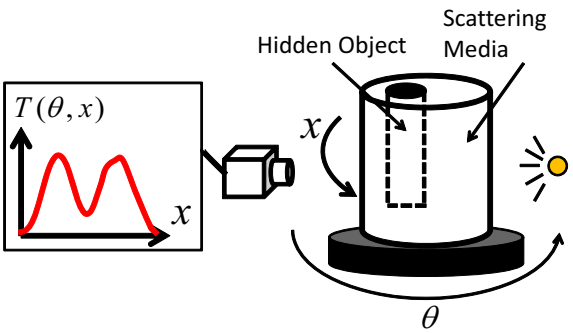

Figure 2: Example of light transport. Light transport $T(\theta, x)$ is a distribution of the ratio based on light angle θ and observed position x. Scattering media are rotated, incident light illuminates the media, and transmitted light is observed

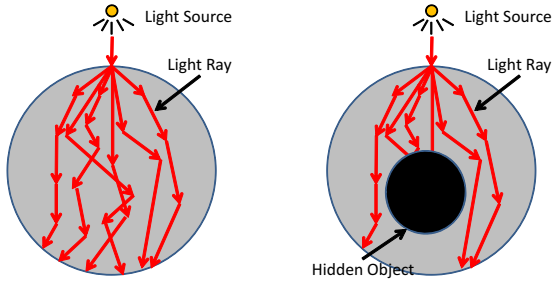

(a) without hidden object (b) with hidden object

Figure 3: Examples of Monte Carlo ray tracing: when the media include objects, some rays are shielded.

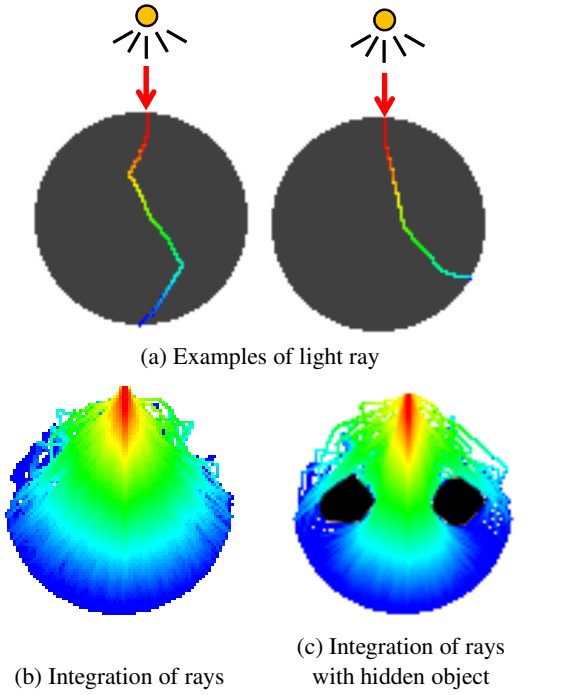

(a) Examples of light ray

(b) Integration of rays (c) Integration of rays with hidden object

Figure 4: Results of Monte Carlo ray tracing: (a) Monte Carlo ray tracing algorithm randomly makes many light paths; (b) example of integration of rays that shows distribution of light power based on ray paths made by Monte Carlo ray tracing; (c) example of integration of rays with shielded objects shown in black.

2 Light Transport in Scattering Media

2.1 Formulation of Light Transport

Figure 1(a) shows an example of scattering media, and (b) shows an image of (a) illuminated by laser light in a darkroom. The objective of this study is to estimate the distribution of hidden objects from the images in Fig. 1(b). The ratio of light that propagates to the observed surface when the incident light falls on the media shown in Fig. 1(b) is called *light transport*. The light that transmits through a scattering media propagates to various sections within the object. Therefore, the light transport provides information about inside the scattering media and the distribution of hidden objects within it.

An example of the observation of light transport on a cross-section of a scattering media is shown in Fig. 2. In this study, the scattering media was rotated by an angle of θ on a rotating table. The light transport can be expressed as one-dimensional distribution $T(\theta, x)$ on observational coordinate x,if θ is determined.

2.2 Monte Calro Ray Tracing

The light transport is the ratio of light that propagates when light is transmitted through a scattering media. If the light ray is determined, the light attenuation ratio at each scattering point can be modeled based on the scattering coefficient, the extinction coefficient, and the phase function that indicates the scattering isotropy[3].

However, even if light enters from the same point, there are many light paths; it cannot be determined uniquely. Under such conditions, various light rays are formed with Monte Carlo ray tracing[7]. Monte Carlo ray tracing allows various light rays to be simulated by randomly varying the angle and distance of rays.

Figure 3(a) shows an example of light rays that were generated in Monte Carlo ray tracing, while (b) shows an example of light rays when hidden objects exist. In Fig. 3(b), the light that was observed below the hidden object contained more scattering light along the sides of the hidden object since it shields the light.

Figure 4(a) shows an actual example of a light ray generated by Monte Carlo ray tracing. Red indicates high intensity and blue indicates low intensity. This example shows that light rays can be randomly generated. Fig. 4(b) shows the averages of the intensities of many generated light rays, while (c) shows ones with hidden objects. The intensity below the hidden object has more blue-level intensities than that without hidden objects because the light that passes around the hidden object is dominant since it is blocked (Fig. 3(b)). This indicates that the intensity changes depending on the existence of the hidden objects.

3 Monte Carlo Voting

3.1 Problem Setting

Our objective is to estimate the distribution of hidden objects within a scattering media from the light transport. Therefore, we also use scattering media that do not contain hidden objects as a reference and estimate those that contain hidden objects.

We assumed that the inside of a scattering media is homogeneous and a hidden object is opaque. The scattering coefficient, the extinction coefficient, and the phase function of a scattering media are uniquely determined if the scattering media material is known. If the material is unknown, then the parameters must be estimated to minimize the error between the observed light transports and the simulated ones by Monte Carlo ray tracing with assumed parameters.

The light transport of a scattering media without hidden objects is defined as $E(\theta, x)$ and that of a scattering media with hidden objects as $T(\theta, x)$. In this study, we do not consider the refraction of light.

3.2 Attenuation Ratio

The light transport of a scattering media contains the information from inside it since it propagates to various sections within the media. Figure 5(a) illustrates an example that a hidden object exists at a center of the scattering media. There are different light transports depending on the existence of hidden objects on the light ray.

Ray-1 that passes through a hidden object is emitted at coordinate x_1 and its $T(\theta, x_1)$ becomes smaller than $E(\theta, x_1)$. Ray-2 that does not pass through the hidden object is emitted at coordinate x_2 and its $T(\theta, x_2)$ nearly equals $E(\theta, x_2)$. Therefore, we focused on the difference in light transport when light passes through a hidden object. The *Attenuation Ratio* (AR), which is a scale to determine whether hidden objects exist on a light ray, is defined by

$$AR(\theta, x) = \frac{T(\theta, x)}{E(\theta, x)}. \quad (1)$$

Calculating the ratio between $T(\theta, x)$ and $E(\theta, x)$ normalizes the light attenuation ratio due to scattering so that the light attenuation ratio caused by a hidden object can be obtained. $AR(\theta, x)$ becomes small if there are hidden objects on rays and close to 1 without them.

3.3 Monte Carlo Voting based on Light Transport

The existence of hidden objects can be estimated by the AR. However, even if light enters from the same point (Fig. 5(a)), there are a huge number of light paths inside media. Therefore, it is difficult to analytically estimate the distribution of the hidden objects from the ARs.

To solve this problem, we propose a new method called Monte Carlo Voting. For cases where analytical estimation is difficult. For the voting process, the scene is expressed as a 2-D array as shown in Fig. 5(b) and (c). This array is used as a voting space. When an AR of a ray is small, the possibility that hidden object exists on the light ray is high. However, the light ray is not unique. Therefore, we vote the AR on all possible light rays which are generated by Monte Carlo ray tracing.

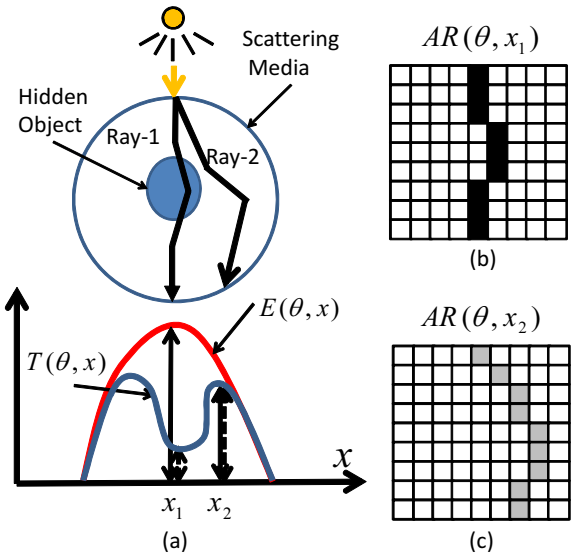

Figure 5: Example of attenuation ratio. Ray-1 is shielded, then small value of AR is voted along Ray-1 as (b). Ray-2 is not shielded, then large value of AR is voted along Ray-2 as (c).

Figure 5(b) and (c) show examples of the voting process. Ray-1 is a randomly sampled path which emits from x_1. Since the $AR(\theta, x_1)$ is small, we can know that hidden objects exist somewhere on the path. Hence, the small value of the AR is voted on the path as Fig. 5(b). On the other hand, Ray-2 is another sampled path which emits from x_2. Since the $AR(\theta, x_2)$ is large, we can know that hidden object does not exist on the path. Hence, the large value of the AR is voted on the path as Fig. 5(c).

By repeating the voting process, the accumulated voting values in the hidden object region become small. If there are enough samples, approximate solutions can be obtained even if the conditions for analytically obtaining the distribution of the hidden objects are not fully met.

4 Experimental Results

4.1 Evaluation by Simulation Data

We experimented using the simulation model described below. The simulation was carried out with incident light from above the scattering media, and observation was carried out below the scattering media. In this case, we assume that all scattering parameters are known.

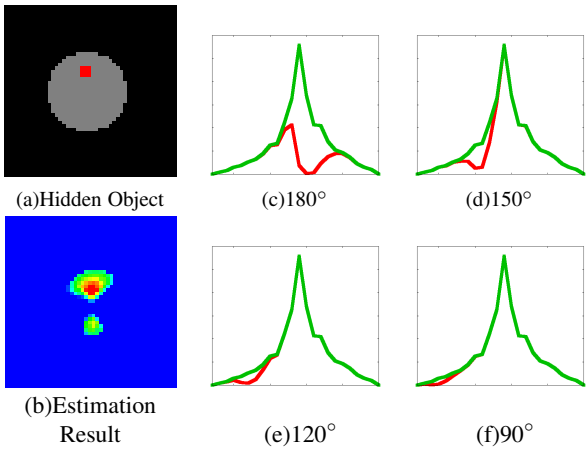

Figure 6: Examples of estimation results and light transport: (a) hidden object in scattering media; (b) estimation result; (c) to (f) light transports of different angles.Green line indicates light transport without hidden object. Red line indicates light transport with hidden object.

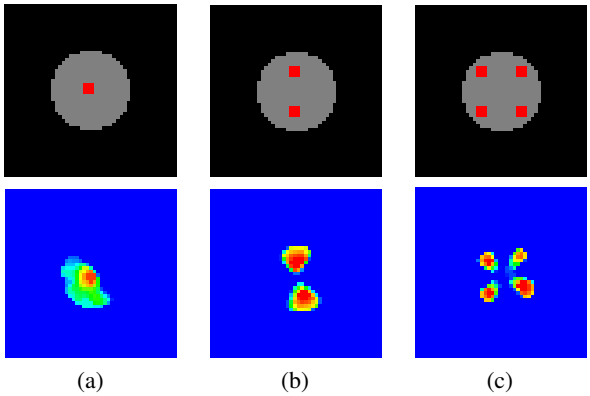

Figure 7: Simulation results. Upper: ground truth. Lower: estimation results. Red region has higher possibility of a hidden object; blue region has lower possibility.

Table 1: Evaluation Results

	(Fig.7 a)	(Fig.6 b)	(Fig.7 b)	(Fig.7 c)
Matching Ratio	88.9%	77.8%	61.1%	52.8%
False Acceptance Ratio	0.75%	0.75%	1.80%	1.39%

Figure 6(a) shows the location of a hidden object as red spot, and (b) shows the estimation results of the distribution of hidden objects. Red color indicates that the possibility of hidden objects is high. Part of the light transport is shown in Figs. 6(c) through (f). In these figures, green and red lines represent $E(\theta, x)$ and $T(\theta, x)$, respectively. Figure 6(c) shows the light transport when the scattering media was turned 180°; in other words, a hidden object was near the observed surface. This shows that part of the light was hidden but scattered light reached the observed surface. From the estimation results of Fig. 6(b), we can see that Monte Carlo Voting can estimate the distribution of the hidden objects at approximately the correct positions.

Subsequently, Fig.7 shows the results when the numbers and the locations of the hidden objects were changed. The comparisons among the results in Figs. 6 and 7 and the ground truth are shown in Table 1. In these experiments, the ratios when the estimated area corresponded to the ground truth (matching ratio) and the area erroneously estimated as a hidden object (false acceptance ratio) in the area other than the ground truth were calculated. When the number of hidden objects was small, the matching ratio accuracy nearly 89%, and the false recognition was scant. This result shows that the proposed method has a high detection performance of foreign substances such as needles in scattering media. On the other hand, when the number of hidden objects was increased, the accuracy degraded accordingly. When there are two or more hidden objects on a ray, the proposed method can not distinguish which hidden objects shielded the ray. This ambiguity causes the accuracy degradation.

4.2 Experimental Setup of Real Object

We experimentally estimated the distribution of hidden objects in an actual environment by a scattering media by mixing milk and agar. The scattering media was a cylinder with 40 mm height and 38 mm diameter. We used a 3 mm diameter wire as a hidden object. Fig. 8(a) shows the actual environment. The scattering media was placed on a rotating stage. A light source is a helium neon laser (632.8 nm). The images were taken in a darkroom with Point Grey Grasshopper camera. The scattering media include one object in Fig. 8(b) and two objects in Fig. 1(a), respectively.

In this experiment, the scattering parameters were obtained using a greedy algorithm. In advance, we capture light transport of the scattering media without shield object. The scattering coefficient, the extinction coefficient and the phase function were changed iteratively until the difference between the light transport of the scattering media and simulation output by Monte Carlo ray tracing is small.

4.3 Experimantal Results by Real Object

We experimented to estimate the distribution of real hidden objects. An example of the light transport is shown in Fig. 9(a). The red line indicates light transport (T) with the hidden object while green line indicates light transport (E) without the hidden object. Since the hidden object is located on the left side, T is smaller than E on the left of the graph.

Figure 9(b) shows the estimation result by our Monte Carlo Voting. The red area indicates high possibility of hidden objects. Figure 9(c) shows the estimation re-

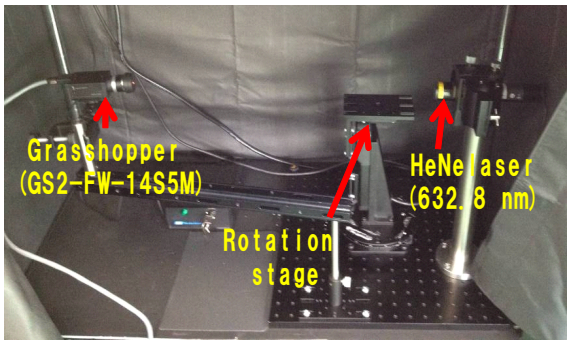

(a)

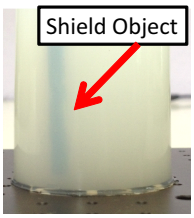

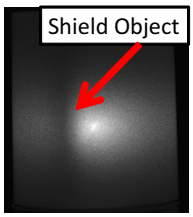

(b) (c)

Figure 8: Experimental setup: (a) in darkroom; (b) hidden object in scattering media; (c) captured image.

sult by conventional back-projection method. Cross-section of the hidden object is a circular. The estimated distribution of the proposed method is a nearly circular. However, the estimated distribution of conventional method was slightly larger , because the conventional method does not consider the physical changes of the light rays due to scattering.

The estimation result of two hidden objects (Fig. 1(a)) is shown in Fig. 1(c). Even with two hidden objects in actual media, their distribution could be estimated Monte Carlo Voting.

When the distributions of the hidden objects were estimated from cross-sections with various heights, a three-dimensional distribution of them can be visualized (Fig. 1(d)). We found two hidden objects with different lengths within the scattering media.

In this experiment, it takes about 30 minutes to capture images (we capture 36 images of object which is rotated 360 degree in 10 degree increments). It takes about 8 hours for Monte Carlo ray tracing with 60,000 samplings, and it takes about 30 minutes for voting process on each height using Intel Core i7 (3.4 GHz) and 8GB memory.

5 Conclusion

We proposed a new scattering tomography called the Monte Carlo Voting. We experimentally verified that our proposed method could estimate the distribution of hidden objects in scattering media.

Future work will improve the measurement accuracy. Our proposed technology approximately obtains the shapes of hidden objects. Some iterative methods have been used in the X-ray CT field. We believe that the accuracy of the estimated shape can be improved by combining such technologies and our method.

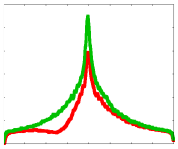

(a) Light Transport

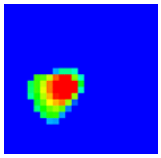

(b) Monte Calro Voting

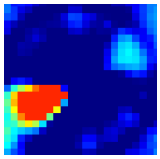

(c) Filtered Back Projection

Figure 9: Comparison with filtered back-projection method: (a) light transport of real scattering media ; (b) result of proposed method; (c) result of conventional method

Acknowledgment

This research is granted by the Japan Society for the Promotion of Science (JSPS) through the "Funding Program for Next Generation World-Leading Researchers (NEXT Program)," initiated by the Council for Science and Technology Policy (CSTP).

References

[1] D. A. Boas, D. H. Brooks, E. L. Miller, C. A. DiMarzio, M. Kilmer, R. J. Gaudette, and Q. Zhang. Imaging the body with diffuse optical tomography. *IEEE Signal Proccessing Magazine*, 18(6):55–75, 2001.

[2] J. Kim, D. Lannan, Y. Mukaigawa, and R. Raskar. Descattering transmission via angular filtering. In *Proc. ECCV2010*, pages 86–99, 2010.

[3] N. Kurachi. *The Magic of Computer Graphics*. CRC Press, 2011.

[4] S. Narasimhan, S. Nayar, B. Sun, and S. Koppal. Structured Light in Scattering Media. In *Proc. ICCV2005*, pages 420–427, 2005.

[5] S. K. Nayar, G. Krihnan, M. D. Grossberg, and R. Raskar. Fast separation of direct and global components of a scene using high frequency illumination. In *Proc. SIGGRAPH2006*, pages 935–944, 2006.

[6] T. Treibitz and Y. Y. Schechner. Active polarization descattering. *Trans. PAMI2009*, 13(3):385–399, 2009.

[7] L. Wang, S. L. Jacques, and L. Zheng. Mcml – monte carlo modeling of light transport in multi-layerd tissues. In *Computer Methods and Programs in Biomedicine 47*, pages 131–146. Elsevier, 1995.